AN INVESTIGATION OF THE EFFECTS OF A SHARP VELOCITY GRADIENT ON THE FLEXURE-TORSION FLUTTER SPEED OF AN AIRFOIL

Edwin G. Dankworth Jr.

Letter on spine: Dankworth

1951

Thesis
D157

Letter on cover:

AN INVESTIGATION OF THE EFFECTS OF A SHARP VELOCITY GRADIENT ON THE FLEXURE-TORSION FLUTTER SPEED OF AN AIRFOIL

Edwin G. Dankworth, Jr.

AN INVESTIGATION OF THE EFFECTS OF A SHARP VELOCITY GRADIENT ON THE FLEXURE-TORSION FLUTTER SPEED OF AN AIRFOIL

Thesis by

Edwin G. Dankworth, Jr.

Lt. Comdr., U. S. N.

In Partial Fulfillment of the Requirements

For the Degree of

Aeronautical Engineer

California Institute of Technology

Pasadena, California

1951

ACKNOWLEDGMENT

The author wishes to express his appreciation to Dr. Y. C. Fung under whose guidance this research was performed, to his co-worker, Lt. D. P. Walker, U.S.N., and to Messrs. Milton Wood, Ace Bartsch, and Marvin Jossey, members of the Guggenheim Aeronautical Laboratory Staff, for their capable technical assistance.

SUMMARY

This report covers the results of an experimental investigation of the effects of a velocity gradient on the flexure-torsion flutter speed of a NACA 0006 airfoil suspended by means of springs.

The presence of the velocity gradient produced no significant change in the speed at which the airfoil commenced normal self-excited oscillations. Oscillations of a torsional nature were found to occur at speeds considerably below the normal flutter speed. The causes of these torsional oscillations were not fully ascertained. It is reasoned however that they were due to flow conditions other than the presence of the velocity gradient.

TABLE OF CONTENTS

I. INTRODUCTION

In References 1 and 2 procedures are given by means of which a critical speed can be computed at which components of an aircraft structure will become unstable. This critical speed is known as the flutter speed. Thus wings, ailerons, vertical and horizontal stabilizers, etc., may be designed so that the flutter speed is well above the maximum speed of the aircraft. Another phenomena, known as buffeting, is not, however, so easily predictable. Buffeting, a type of forced oscillation of an aircraft structural component, is ordinarily associated with the vorticity present in the wing wake or propeller slipstream. Design procedures by means of which buffeting may be eliminated or reduced in intensity are well known but theories for predicting its occurrence are incomplete.

Lo, in Reference 3, notes that the nature of the wing wake has not been completely established. Abdrashitov, in Reference 4, approximates the effect of the wing wake on the tail by a harmonic disturbance force but this has not satisfactorily explained buffeting phenomena. Lo, loc. cit., approximates the wing wake by a surface of discontinuity which he calls an interface. Across this interface finite velocity and density changes occur and he determines the effects of this interface on an airfoil. His assumptions are as follows:

1. The interface is flat, of zero thickness, and tends to infinity in all directions.

2. The airfoil surface is of infinite aspect ratio, is of small thickness relative to the chord, and has a mean position parallel to the interface.

3. The oscillatory motion of the wing is two-dimensional, periodic, and is of small amplitude relative to the chord.

4. The flow is incompressible and non-viscous.

He finds that the effect of this interface is to reduce the conventional flutter speed and to cause a new flutter phenomena to occur at a greatly reduced speed. In a specific example, with the interface located in the plane of the airfoil, he finds that instabilities occur at speeds of approximately 90% and 3% of the conventional flutter speed.

An attempt was made in this investigation to obtain experimental corroboration of Lo's results and for this purpose a wind tunnel set up was designed to provide conditions which corresponded as closely as possible to Lo's assumptions. It was realised that an interface such as Lo postulated was unobtainable because of the viscous nature of gases and therefore this investigation can not be regarded as demonstrating that Lo's theoretical approach was incorrect. It should rather be regarded as an attempt to discover if the presence of the velocity gradient in the neighborhood of the airfoil would lower the flutter speed sufficiently so that buffeting should be regarded as a flutter phenomena. If the latter hypothesis is shown to be incorrect then a more plausible approach is to consider buffeting as the response of an elastic system to a turbulent flow with statistical methods providing the most suitable mathematical procedures for handling the problem. Then the shear flow nature of the flow field will only be reflected in the calculation of the mechanical admittance.

The velocity discontinuity obtained in this investigation was of the nature of a boundary layer and consisted of a region across which

the magnitude of the flow velocity varied from that of the free stream to a greatly reduced value. The surface of the discontinuity adjacent to the airfoil, i.e., the free-stream edge of the so-called boundary layer, was quite distinct, however, and was very nearly parallel to the plane of the airfoil. Within this region the sharpness of the velocity gradient varied, becoming less steep with down-stream distance. On the average, the flow velocity was reduced by 30% at stations ½ inch from the surface of the discontinuity. It should be pointed out that this velocity gradient, while not approaching Lo's interface in sharpness, was considerably steeper than any which would be found in the wake of a wing or fuselage.

II. DESCRIPTION OF APPARATUS

An open-return wind tunnel, as described in Reference 5, and shown schematically in Figure 1, was used for this investigation. Power was supplied by a conventional automobile engine with a maximum output of 125 h.p. which drove an eight bladed propeller through a transmission system with three gear ratios. The throttle was actuated by a reversible d.c. motor which in turn was controlled remotely by a two way switch thus permitting tunnel velocity variations to be achieved from a position adjacent to the test section.

To insure steady flow through the test section, a set of screens was mounted at the entrance to the contraction section. Two of the screens were made of cheese cloth, while the third was made of 20 mesh copper screening. To prevent oscillations of the engine-propeller section from being transmitted to the test section a 1½ inch gap was left between the diffuser section and the fan section.

A maximum speed of about 65 feet per second and a minimum speed of about 10 feet per second were obtainable in the test section.

The speed controlling mechanism was not entirely adequate particularly for test-section velocities between 0 and 20 and between 45 and 60 feet per second, the speed ranges within which this investigation was largely conducted. The attainment of a desired velocity to within 0.5 feet per second was frequently a time-consuming process due to the time lag between throttle actuation and response of the engine. Speed variation for a given throttle setting was also frequently encountered.

The airfoil, mounted vertically in the test section was attached at either end to steel springs by means of clamps. The mounting system

is shown in Figures 2 and 3. The springs, of 1/2" x 1/16" cross-section, passed through slots in the upper and lower tunnel walls, and were clamped to heavy steel clamp supports. The airfoil was thereby given two degrees of freedom. It could move in a direction perpendicular to its own plane and rotate about one axis through the centerline of the springs. No tendency was observed, even when the airfoil was agitated by hand, for its motion to be other than two-dimensional. In order to maintain a constant tension on the springs, the lower clamp consisted of a horizontal spring flexure which permitted a considerable variation in vertical dimensions of the test section to occur with little change in spring characteristics.

The NACA 0006 airfoil was of laminated wood construction with a 9 inch chord and 35 inch span. The curve of lift coefficient versus the angle of attack is given in Figure 4. The clamps at either end were faired smoothly into the contour and provided sufficient clamping action to withstand a vertical end load of more than 75 lbs. The pertinent physical constants of the spring-airfoil system are given in the Appendix.

In order to stop the violent oscillations of the airfoil when they occurred restraining bars were provided which could be used to force the springs against the tunnel wall slot, thereby providing a positive restraint against airfoil motion.

Two sets of strain gages were attached to the upper spring, one set mounted parallel to the spring axis and the other set mounted at 45 degrees to the axis. The parallel set measured bending strain primarily while the skewed set, by means of the proper electrical connection, measured torsional strain. It was not possible to separate completely

the two types of strain, particularly in the parallel set. However, satisfactory results were obtained since the primary purpose of the strain gages was that of frequency determination. The output of the gages was fed through an amplifier to a Heiland Type A400 R-6 recording oscillograph. The oscillations thus appeared as sine waves on a recording tape on which timing lines spaced .01 seconds apart also appeared. Thus the determination of the frequency of vibration was a simple matter. Sample recordings for several types of oscillation are shown in Figure 5.

The formation of the velocity gradient was accomplished by means of the installation of a sheet aluminum covered shape in the test-section. This shape, which will hereafter be called the "barrier", was designed so that it could be easily removed from the test section, and could be moved both fore-and-aft and sidewise within the test-section. A plan view of the test-section with barrier and airfoil installed is given in Figure 6.

Throughout the investigation the angle of attack of the airfoil was maintained at zero degrees with respect to the tunnel axis. This was set originally by mounting the airfoil in its clamps and then sighting along bench marks on the test-section floor and ceiling. The clamp supports were adjusted until perfect alignment was obtained. Sidewise and fore-and-aft alignment was accomplished in the same manner. Clamps were adjusted so that a spring length of 7.5 inches was obtained.

III. TEST PROCEDURE

A velocity survey of the working section of the tunnel with the barrier and airfoil removed is presented in Figure 7. A velocity survey of the tunnel with barrier installed is given in Figures 8 and 9 for two test-section velocities. Tuft surveys of the region outside the barrier boundary layer were also conducted. No deviation from flow parallel to the airfoil chordline was detectable in the higher speed case. Measurements were, however, insufficiently precise to detect variations of less than five degrees. For the lower speed the tuft method was completely inadequate because of the insufficient velocity of flow.

With tunnel velocity zero the natural frequencies of oscillation of the flexural and torsional modes were determined. The effect on the frequencies of the added tension in the springs was determined by hanging weights on the lower spring. Because of the dynamic coupling between the torsional and flexural modes of oscillation, it was found to be impossible to excite one mode without exciting the other and hence to obtain direct oscillograph recordings of the two frequencies. Figure 5(d) shows the effect of coupling on strain gage response. It was noted that the node, i.e., the point about which the airfoil oscillated as if it had only a torsional degree of freedom, could be easily located and that the airfoil could be caused to oscillate about the node. The node location was found and the frequency of oscillation recorded on the oscillograph. By means of a procedure given in the Appendix the fundamental frequencies were deduced from these data. The results are plotted in Figures 10, 11, and 12.

The flutter speed with and without the barrier installed was determined using similar procedures. Two definitions of flutter speed were used. The first was the lowest tunnel speed at which the airfoil broke into such violent oscillations that the springs struck the sides of the slots through which they passed. The second definition gave the flutter speed as the lowest speed at which the airfoil commenced small regular oscillations. As would be expected the two criteria gave somewhat different results and are discussed in the following section.

Flutter speeds were determined for the zero tension condition with the barrier in several different fore-and-aft positions. A control flutter speed was established prior to the installation of the barrier and checked when the barrier was removed. Results of a number of runs are plotted in Figure 13. During two runs of this type the flutter frequency was determined. Results are also plotted in Figure 13.

It was early seen that the athwartships location of the airfoil and barrier as shown in Figure 6 was the optimum one in-so-far as this position places the airfoil as close to the velocity gradient as is practical without undue interference from the boundary layer. Tests also showed that moving the barrier inboard had no noticeable effect on flutter speed.

Flutter speeds were also determined with weights hung on the lower spring. For two sets of runs the barrier was removed and for another set the barrier was located one-half chord length ahead of the airfoil leading edge. Results are plotted in Figure 14.

IV. DISCUSSION OF RESULTS

Figures 8 and 9 show the velocity profiles which occurred at several stations within the test section and also the boundaries of the velocity discontinuity which are described by lines of constant velocity.

Inspection of these figures reveals that the attempt to create a sharp velocity discontinuity in the airflow was fairly successful, particularly at the higher tunnel speed. Figure 8 shows that within a range of ½ inch the velocity has changed 30% or more. A comparison of Figure 8 with Figure 9 shows the decrease in sharpness of the velocity gradient which accompanied the decrease in tunnel speed. Although the proper equipment for studying the degree of turbulence within the region of the airfoil was unavailable, tests with the type of hotwire being used by MacCready and Madden of CALCIT in their study of atmospheric turbulence failed to show any turbulence except in the wakes of the airfoil and barrier and in the neighborhood of the airfoil when the airfoil was oscillating violently. The apparatus had a time constant of 0.01 seconds, however, and thus would only indicate turbulence of relatively large scale. The previously mentioned tuft surveys showed that the airflow past the airfoil was fairly straight although it is possible that the airfoil was at some slight angle of attack when the barrier was in place.

The curves of Figure 12 demonstrate the close agreement between theoretical and experimental frequency determination especially when the springs were under zero tension, and also the manner in which the frequencies changed under tension. It should be noted that the torsional

frequency was constant under the load while the flexural frequency increased. The effect of the resulting increase of the ratio of the two frequencies on flutter speed may be seen in Figure 14. This figure shows that the flutter speed reached a minimum when the frequency ratio was approximately one. The theoretical curves of Figure 12 were obtained from equations as derived in the Appendix. The discrepancy which exists between the experimental and theoretical curves under load conditions can be explained by changes in the relative degree of clamping. As was stated previously, it was found to be impossible to determine the torsional and flexural frequencies by direct measurement due to the dynamic coupling between the two degrees of freedom. Instead the location of the node point and the frequency of vibration about the node was recorded. These data are plotted in Figure 10. The frequency curve (solid) in Figure 10 as plotted can be regarded as the mean between two curves (dotted). The data should have fallen on a smooth curve since the accuracy of frequency determination was of a high order. The fact that almost all the experimental points lie within a definite area and form a pattern within the area seems to indicate that the degree of clamping was not fixed but varied between two limits. The mean frequency curve was used to calculate the two natural frequencies. (See Appendix.) The clamping problem was early recognized as being of great importance and several methods were used in attempts to gain greater uniformity in clamping action. Toward the end of the experimental work the clamps were even redesigned as shown in Figure 3, but difficulties persisted and no satisfactory solution was found.

Flutter speed is defined as the lowest speed at which an airfoil

with a specified number of degrees of freedom will become unstable. In this investigation, a fairly wide range of speeds were found, on the order of 10 feet per second within which oscillations would start of themselves, build up to a stable amplitude, and die out upon reduction of speed. The maximum flexural amplitude was limited by the width of the slots in the tunnel walls and when this amplitude was reached a different, more violent type of oscillation was found to occur which was characterized by large torsional amplitudes and by the springs striking the tunnel walls with considerable force. This type of oscillation, unlike the more normal type, would not die out of itself until the tunnel speed was reduced to a value 10 feet per second less than the minimum speed at which even the slightest oscillations were noticeable.

An explanation of this phenomenon is suggested by Chuan in Reference 6. This author points out that when an airfoil, initially at low angles of attack, is stalled and unstalled periodically, the shedding of vortices must be periodic and have the same period as the oscillations, and that this type of oscillation, once started, is no longer controlled by the stationary angle of attack and flow velocity but by the shedding frequency. This would seem to apply to the case under discussion since the torsional amplitude was on the order of 15-20 degrees, well above the stalling angle of attack of the NACA 0006 section. It also explains why the oscillations continued even when the tunnel speed was reduced to a point a good deal below which self-excited oscillations would begin.

At first the lowest speed at which these violent oscillations took place was used as the criterion for flutter because it was relatively definite and because the striking of the tunnel walls by the spring could

be both seen and heard. However, the experimental determination of the natural frequencies permitted an accurate theoretical calculation of the flutter speed to be made, (see Appendix) and it was found that the speed of violent oscillations was 15-20 feet per second higher than the predicted value. Also, due to the high angles of attack, a portion of the airfoil surface penetrated into the region of rapidly changing velocity during part of each cycle. It was therefore decided to use as the flutter speed the lowest speed at which the smallest, regular oscillations would occur. This was also a good deal higher than the predicted value, as can be seen in Figure 13, but approached it more closely and had the advantage that it corresponded better with the usual definition of flutter speed.

The main disadvantage to this criterion lay in its indefiniteness. It was frequently difficult to determine whether or not the small motions of the airfoil were regular or whether they were intermittent and caused by turbulence in the airflow. This was particularly true when the barrier was in place. Although it was not felt that the turbulence was excessive the effect of small flow perturbations at speeds close to the flutter speed was sufficient to send the airfoil into oscillations which died out relatively slowly. An attempt was made to analyze signals from the strain gages in an oscilloscope but it was found that the signals which corresponded to small oscillations of the system required amplification in order to become of any value. Equipment which would do this and which would also filter out extraneous signals from such sources as the engine ignition system was unavailable.

In the light of the foregoing arguments it is believed that the

rather wide range of speeds at which flutter would occur is explained. In spite of a good deal of care it was not possible to fix the degree of clamping or to determine the speed at which small oscillations occurred with any degree of precision. The effect of these variables is evident in Figure 13. The large number of points which were plotted are the result of several runs during all of which the configuration of the system was kept constant. This indeterminacy was unfortunate since Lo's results indicated that if the velocity gradient did have an effect on the conventional flutter speed, it would be relatively small.

It is to be noted that other investigators appear to have had similar difficulties. Figure 15, reproduced From Figure 15 of Reference 3, shows a range of experimental flutter speeds for a given value of the natural frequency ratio rather than any definite speed. An examination of Figure 15 also shows that the experimental flutter speeds were always greater than the theoretical value by amounts averaging 15% of the theoretical value. This may be compared with an average flutter speed 27% higher than the theoretical value as determined in this investigation. The explanation given in the reference is that the influence of internal friction, not taken into account in the theoretical calculations, is much greater, relatively speaking, in systems designed to flutter at low speeds, than it is in actual practice where structures flutter at much higher speeds. Internal friction will always tend to raise the flutter speed.

In this investigation there were, in addition to the internal friction, two other conditions which would tend to raise the flutter

speed above the theoretical value as calculated. The theoretical calculations were made considering the aerodynamic forces to be constant across the span. In the experiment the effect of the finite span would be to decrease the forces acting on the tip section and hence the total aerodynamic forces acting on the airfoil per unit length of span. In addition the airfoil tips were probably in the tunnel wall boundary layer thus further decreasing the aerodynamic forces. It is believed that the foregoing consideration explains in a qualitative manner at least the reason for the large discrepancy between theoretical and experimental flutter speed.

It is evident then from Figures 13 and 14 that within limits of experimental accuracy no evidence was discovered which would indicate that the presence of the velocity gradient had any effect on flutter speed.

Lo, in Reference 3, found that a region of instability might possibly exist at very low speeds, in which oscillations of a predominantly flexural nature would occur. At tunnel speeds between zero and 10 feet per second with the trailing edge of the barrier between 3/4 and 1 chord length ahead of the leading edge of the airfoil, oscillations of large amplitude did take place. These oscillations were, however, predominantly torsional in nature, occurred at the natural torsional frequency of the system, and ceased completely when the tunnel speed was changed by ± 2 feet per second or when the barrier was moved closer to the airfoil. There was insufficient time or equipment available to study in detail the flow conditions which accompanied these oscillations, but it is not

believed that they were due to the presence of the velocity gradient. Flow conditions in back of the barrier make it likely that the airfoil was actually at some fairly large angle of attack and that the oscillations were due to vortex shedding. The use of Tyler's formula, $\frac{nb \sin \alpha}{V} = K$, given in Reference 7, and assuming a value of ~~45~~ 20 degrees for α gives a value of $K \cong .14$. (See Appendix.) This is in very close agreement with Tyler's average value of $K = .15$ for airfoils and also with Chuan's results in Reference 6. Further investigation is required to determine precisely the causes of this phenomenon.

V. CONCLUSIONS

This investigation failed to reveal any significant variations in airfoil flutter speed which could definitely be attributed to the presence of the velocity discontinuity. Although oscillations were observed which occurred at tunnel velocities much lower than those at which conventional flutter took place, it is believed that these were due to causes other than the velocity discontinuity. It is therefore believed that Lo's results reflect the idealization of the flow into an interface rather than any physical causes of buffeting or flutter. The negligibly small changes in the flutter speed point further to the fact that the effect of the velocity gradient, of the order of magnitude likely to occur in practice, is small, so that it is sufficiently accurate to use the aerodynamic coefficients measured in a uniform flow in the estimation of the mechanical admittance. Such coefficients being well known, it is concluded that the only relevant data one must have in order to analyze tail buffeting is the turbulence in the flow in the region of the tail, i.e., the turbulence power spectrum and the correlation functions.

This investigation, and all the remarks made above, are concerned only with low speed phenomena. Buffeting due to unstable shock waves is of different origin and is not dealt with here.

REFERENCES

1. Theodorsen, T., "General Theory of Aerodynamic Instability and the Mechanism of Flutter", NACA Report No. 496, (1940).

2. Theodorsen, T., and I. Garrick, "Mechanism of Flutter — A Theoretical and Experimental Investigation of the Flutter Problem", NACA Report No. 685, (1940).

3. Lo, Shih-Chun, "Oscillating Airfoil in Parallel Streams Separated by an Interface", CALCIT Thesis, (1950).

4. Abdrashitov, G., "Tail Buffeting", NACA Technical Memorandum No. 1041, (1943).

5. Dunn, L. G. and M. Finston, "Self-excited Oscillations of Airfoils", Report in Final Fulfillment of Contract NAw 2329, (April, 1945), California Institute of Technology.

6. Chuan, R. L., "An Investigation of Vortex Shedding as Related to the Self-excited Torsional Oscillation of an Airfoil", CALCIT Thesis, (1948).

7. Goldstein, S., "Modern Developments in Fluid Dynamics", University Press, Oxford, England, (1938), Vol. II, Chapter XIII.

8. Timoshenko, S., "Strength of Materials", Second Edition, Van Nostrand and Company, (1940), Vol. I, Section 60.

APPENDIX

CALCULATIONS

I. AIRFOIL AND SPRING CONSTANTS

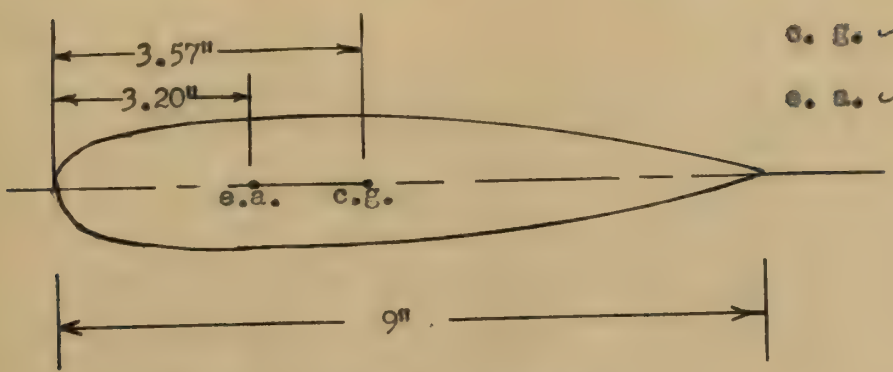

c. g. ∽ center of gravity

e. a. ∽ elastic axis

Weight of airfoil = 3.7780 lbs.

Mass of airfoil = 9.79×10^{-3} $\frac{\text{lb. sec.}^2}{\text{in.}}$

Radii of gyration

about c. g. = 3.113"

about e. a. = 3.25"

Length of spring = 7.5"

Cross-section of springs = 1/16" x 1/2"

Mass of spring ∽ 1.73×10^{-4} lb. $\frac{\text{sec.}^2}{\text{in.}}$

Total spring mass ∽ 3.46×10^{-4} lb. $\frac{\text{sec.}^2}{\text{in.}}$

II. DETERMINATION OF NATURAL FREQUENCIES OF VIBRATION

A. Flexural Frequency

1. Differential Equation

The following configuration is assumed in which the springs are built in at both ends and the airfoil is considered stiff as compared to spring.

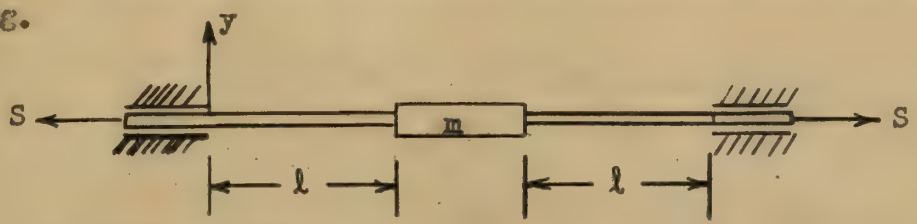

Considering the equilibrium of a differential length of spring,

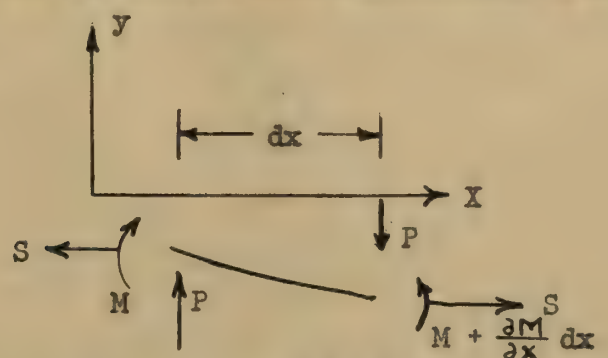

$$\Sigma_M = 0 = M + Pdx - \left(M + \frac{\partial M}{\partial x}\,dx\right) - S(-dy)$$

$$Pdx - \frac{\partial M}{\partial x}\,dx + S\,dy = 0$$

Assume $$\frac{dM}{dx} = EI\,\frac{d^3y}{dx^2}$$

Then the differential equation is

$$EI\,\frac{d^3y}{dx^3} - S\,\frac{dy}{dx} - P = 0$$

This has the solution

$$y = C_2 \cosh qx + C_3 \sinh qx - \frac{Px + C_1}{S}$$

where

$$\frac{S}{EI} = q^2$$

The boundary conditions are

$$y = 0 \quad \text{at} \quad x = 0$$

$$\frac{dy}{dx} = 0 \quad \text{at} \quad x = 0$$

$$\frac{dy}{dx} = 0 \quad \text{at} \quad x = l$$

Substituting the boundary conditions into the equation for y gives

$$y = -\frac{P}{Sq}\,\frac{\cosh ql - 1}{\sinh ql}\cosh qx + \frac{P}{Sq}\sinh qx - \frac{Px}{S} + \frac{P}{qS}\,\frac{(\cosh ql - 1)}{\sinh ql}$$

When $x = l$

$$y = -\frac{Pl}{S} + \frac{2P}{Sq}\left[\frac{\cosh ql - 1}{\sinh ql}\right]$$

Taking limit as q approaches zero

$$y = -\frac{Pl}{S} + \frac{2P}{Sq}\,\frac{\left[1 + \frac{ql^2}{2} + \frac{ql^4}{24} - 1\right]}{\left[ql + \frac{(ql)^3}{6}\right]}$$

$$= -\frac{Pl}{S} + \frac{Pl}{S}\left[1 - \frac{(ql)^2}{12}\right]$$

Putting $q^2 = \frac{S}{EI}$

$$y = -\frac{Pl^3}{12EI}$$

This agrees with the deflection found by setting $S = 0$ in the differential equation.

The spring constant in flexure is then, taking into account both

springs

$$K_h = \frac{2P}{Y} = \frac{2}{\frac{l}{S}\left[1 - \frac{2}{ql}\left(\frac{\cosh ql - 1}{\sinh ql}\right)\right]}$$

As an example K_h is worked out for S = 40 lbs.

The cross-section of the springs is

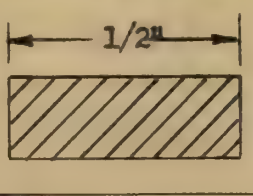

$E = 30 \times 10^6 \frac{lb.}{in^2}$

$I = \frac{bh^3}{12}$

$$q = \sqrt{\frac{S}{EI}} = \sqrt{\frac{40}{30 \times 10^6 \times \frac{1}{12 \times 2 \times 16^3}}} = .362$$

The length of each spring is 7.5".

$$ql = 7.5 \times .362 = 2.71$$

$$K_h = \frac{2}{\frac{7.5}{40}\left[1 - \frac{2}{2.71}\left(\frac{7.55 - 1}{7.48}\right)\right]} = 30.01$$

The flexural frequency, ω_h , is then:

$$\omega_{h_{40}} = \sqrt{\frac{K_h}{m}} = \sqrt{\frac{30.01}{9.79} \times 10^3}$$

$$= 55.5 \text{ rad./sec.}$$

This may be compared with ω_h for zero tension on the spring.

$$\omega_{h_0} = 42.2 \text{ rad./sec.}$$

2. Energy Method

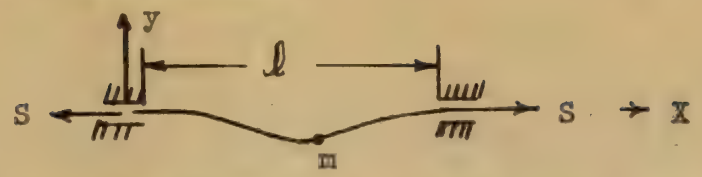

Assume a deflection curve shown above. In this case, let l be the length of both springs.

$$y = y_o \sin^2 \frac{\pi x}{l}$$

This satisfies all boundary conditions.

a. The potential energy due to bending moments:

$$V_1 = \frac{1}{2} \int_o^l M \frac{d^2y}{dx^2} dx \qquad M = EI \frac{d^2y}{dx^2}$$

b. The potential energy due to loads:

$$V_2 = \frac{S}{2} \int_o^l \left(\frac{dy}{dx} \right)^2 dx$$

c. The kinetic energy of vibrating spring particles:

$$T_1 = \frac{y_o^2 \rho A \omega^2}{2} \int_o^l \sin^4 \frac{\pi x}{l} dx$$

ρ = spring density

A = Area of Spring

d. The kinetic energy of the airfoil:

$$T_2 = \frac{1}{2} m \omega^2 y_o^2$$

Performing the indicated integration and equating potential and kinetic energies

$$\omega^2 = \frac{\frac{EI\pi^4}{l^3} + \frac{S\pi^2}{4l}}{\frac{3ms}{16} + \frac{m}{2}}$$

The mass of the springs may be neglected since it is only 1/30 of the mass of the airfoil. For S = 40 lbs.

$$\omega_h^2 = \frac{\frac{30 \times 10^6 \times \pi^4}{(15)^3 \times 12 \times 2 \times (16)^3} + \frac{40 \times \pi^2}{4 \times 15}}{.00979}$$

$$\omega_{h_{40}} = \sqrt{\frac{(8.80 + 6.58)\,2}{.00979}}^2$$

$$\omega_{h_{40}} = 56.2 \text{ rad/sec.}$$

The curves of flexural frequencies versus spring tension are plotted on Figure 9.

B. Torsional Frequency

It is assumed that increases in spring tension produces only second order effects on the torsional spring constant.

From Reference 7,

$$K_\alpha = \frac{\beta b c^3 G}{L}$$

where β is a constant depending on the dimensions of the cross section

b ~ long dimension

c ~ short dimension

In this case, $\beta = .307$

$$K_\alpha = \frac{.307 \times \frac{1}{2} \times \left(\frac{1}{16}\right)^3 \times 1.1 \times 10^7 \times 2}{7.5}$$

= 110.1 in. lb.

$$\omega_\alpha = \sqrt{\frac{K_\alpha}{I_{E.a.}}} = \sqrt{\frac{1.1 \times 10^2}{3.18 \times 10^{-2}}}$$

= 59 rad./sec.

C. Natural Frequency Determination by Experimental Means

The experimental data is plotted in Figure 8.

Consider the following system

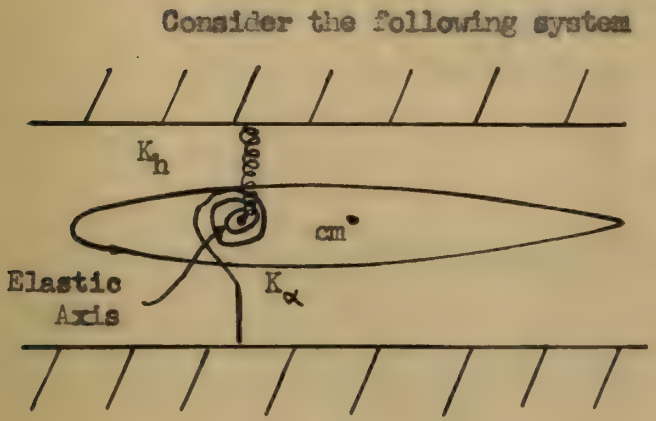

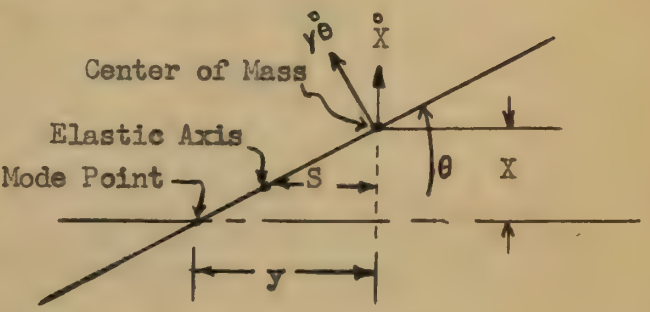

For small oscillations of the above system, the following equations will apply

Potential energy: $$V = \frac{K_h (S\theta - x)^2}{2} + K\alpha \frac{\theta^2}{2}$$

Kinetic energy: $$T = \frac{m\dot{x}^2}{2} + \frac{I\dot{\theta}^2}{2}$$

Using La Grange's equations

$$I\ddot{\theta} + K_h S^2 \theta - K_h S x + K_\alpha \theta = 0$$

$$m\ddot{x} - K_h S \theta + K_h x = 0$$

The following assumptions are made:

a. $\theta = \theta\, e^{i\omega t}$

b. $x = x\, e^{i\omega t}$

c. $\omega_h^2 = \frac{K_h}{m}$

d. $\omega_\alpha^2 = \frac{K_\alpha}{I}$

Assumptions "c" and "d" are valid if the mass of the springs is small compared to m. The condition for a node at y is

$$y = \frac{x}{\theta} \qquad \text{or} \qquad y = -\frac{x}{\theta}$$

Complete experimental results were obtained for a range of node points such that $y = -\frac{x}{\theta}$. The equations then reduce to two simultaneous equations for ω_α and ω_h.

$$\omega_h^2 = \frac{\omega^2}{1 + \frac{s}{y}}$$

$$\omega_\alpha^2 = \omega_h^2 \frac{m}{I}(-ys - s^2) + \omega^2$$

where w is the frequency of oscillations about the node.

Solutions of the above equations for ω_h and ω_α as a function of spring tension are plotted in Figure 9. Note that ω_α is independent of spring tension.

III. FLUTTER SPEED DETERMINATION

The procedure and symbols used are in accordance with those defined in References 1 and 2.

W_{T_1} = 3.7780 # = .1174 $\frac{\#\ sec.^2}{ft.}$ = .00979 $\frac{\#\ sec.^2}{ins.}$

K_o^2 = 6.723

$r_{c.g.}^2$ = 3.113

$r_{e.a.}^2$ = 3.249

a = -.289 a^2 = .0835 $\frac{1}{2} + a$ = .211 $\frac{1}{2} - a$ = .789

x_α = .0822

K = .0261 $\sqrt{K}$ = .16156

r_α^2 = .1605 r_α = .4006

ω_α = 54.4 ω_α^2 = 2959

ω_h = 41.5 ω_h^2 = 1722

A_{α_1} = 6.358

A_{α_2} = .789

A_{h_1} = 3.438

C_{α_1} = 3.438

C_{α_2} = 1.000

C_{h_1} = 39.314

A_1 = 238.138

B_1 = -2.174

C_1 = 10.733

D_1 = -27.581

Ω_α = 1.000

Ω_h = 3.6259

Real Equation

$$A_r X^2 + B_r X + C_r = 0$$

Imaginary Equation

$$A_i X^2 + B_i X + C_i = 0$$

Where

$$A_r = \Omega_h \Omega_\alpha$$

$$B_r = \Omega_h R_{a_\alpha} + \Omega_\alpha R_{c_h}$$

$$C_r = A_1 + B_1 \frac{2G}{K} + C_1 \frac{2F}{K^2}$$

$$A_i = 0$$

$$B_i = \Omega_h I_{a_\alpha} + \Omega_\alpha I_{c_h}$$

$$C_i = \frac{1}{K}\left(D_1 + C_1 \frac{2G}{K} - B_1 2F\right)$$

$$R_{a_\alpha} = -A_{\alpha_1} + \left(\tfrac{1}{4} - a^2\right)\frac{2G}{K} - \left(\tfrac{1}{2} + a\right)\frac{2F}{K^2}$$

$$R_{c_h} = -C_{h_1} - \frac{2G}{K}$$

$$I_{a_\alpha} = \frac{1}{K}\left[A_{\alpha_2} - \left(\tfrac{1}{2} + a\right)\frac{2G}{K} - \left(\tfrac{1}{4} - a^2\right)2F\right]$$

$$I_{c_h} = \frac{1}{K}\,2F$$

$$X_R = \frac{-B_R \pm \sqrt{B_r^2 - 4A_R C_R}}{2AR}$$

$$I_I = -\frac{C_i}{B_i}$$

From Theodorsen

$\frac{1}{K}$	F	-G	$-\frac{2G}{K}$	$\frac{2F}{K^2}$	2F
2.000	.5979	.1507	.6028	4.7832	1.1958
2.273	.6136	.1592	.7236	6.3326	1.2272
2.500	.6250	.1650	.8250	7.8125	1.2500

$1/\sqrt{\bar{X}} = 2.000$

R_{a_α}	=	-7.4676	A_R	=	3.6259	A_i	= 0
R_{c_h}	=	-38.7112	B_R	=	-65.7880	B_i	= 7.5919
I_{a_α}	=	1.4342	C_R	=	290.7866	C_i	= -62.9024
I_{c_h}	=	2.3916	X_i	=	8.2855	X_r	= 7.6191 & 10.5248

$1/\sqrt{\bar{X}} = 2.273$

R_{a_α}	=	-7.815	A_R	=	3.6259	A_i	= 0
R_{c_h}	=	-38.590	B_R	=	-66.9264	B_i	= 8.8660
I_{a_α}	=	1.676	C_R	=	307.679	C_i	= -74.281
I_{c_h}	=	2.799	X_i	=	8.3782	X_r	= 8.6604 & 9.7975

$1/\sqrt{\bar{X}} = 2.500$

R_{a_α}	=	-8.144	A_R	=	3.6259	A_i	= 0
R_{c_h}	=	-38.489	B_R	=	-68.0183	B_i	= 9.9689
I_{a_α}	=	1.8875	C_R	=	323.7831	C_i	= -84.296
I_{c_h}	=	3.125	X_i	=	8.4559	X_r	= Complex

The $\bar{X}_i$ and $\bar{X}_r$ are plotted in Figure 16. The intersection of the X_i and X_r curves give

$$\omega = \frac{r_\alpha \omega_\alpha}{\sqrt{K}\sqrt{\bar{X}}} = 46.5 \text{ cyc/sec} \qquad V = \frac{r_\alpha \omega_\alpha b}{\sqrt{K}} \frac{1}{\bar{K}} \frac{1}{\sqrt{\bar{X}}} = 39.4 \text{ ft./sec.}$$

IV. TYLERS FORMULA

$$\frac{N b \sin \alpha}{V} = K$$

N = Natural frequency of torsional oscillation in cycles/sec

b = Chord of airfoil in feet

α = Angle of attack of airfoil

V = Flow velocity

$$\frac{\frac{54}{2\pi} \cdot \frac{3}{4} \cdot \sin 20^\circ}{16} = .138$$

Note that Goldstein, Reference 7, defines the above formula as $\frac{Nb'}{V} = K$ where b' is the width of the body perpendicular to the direction of flow.

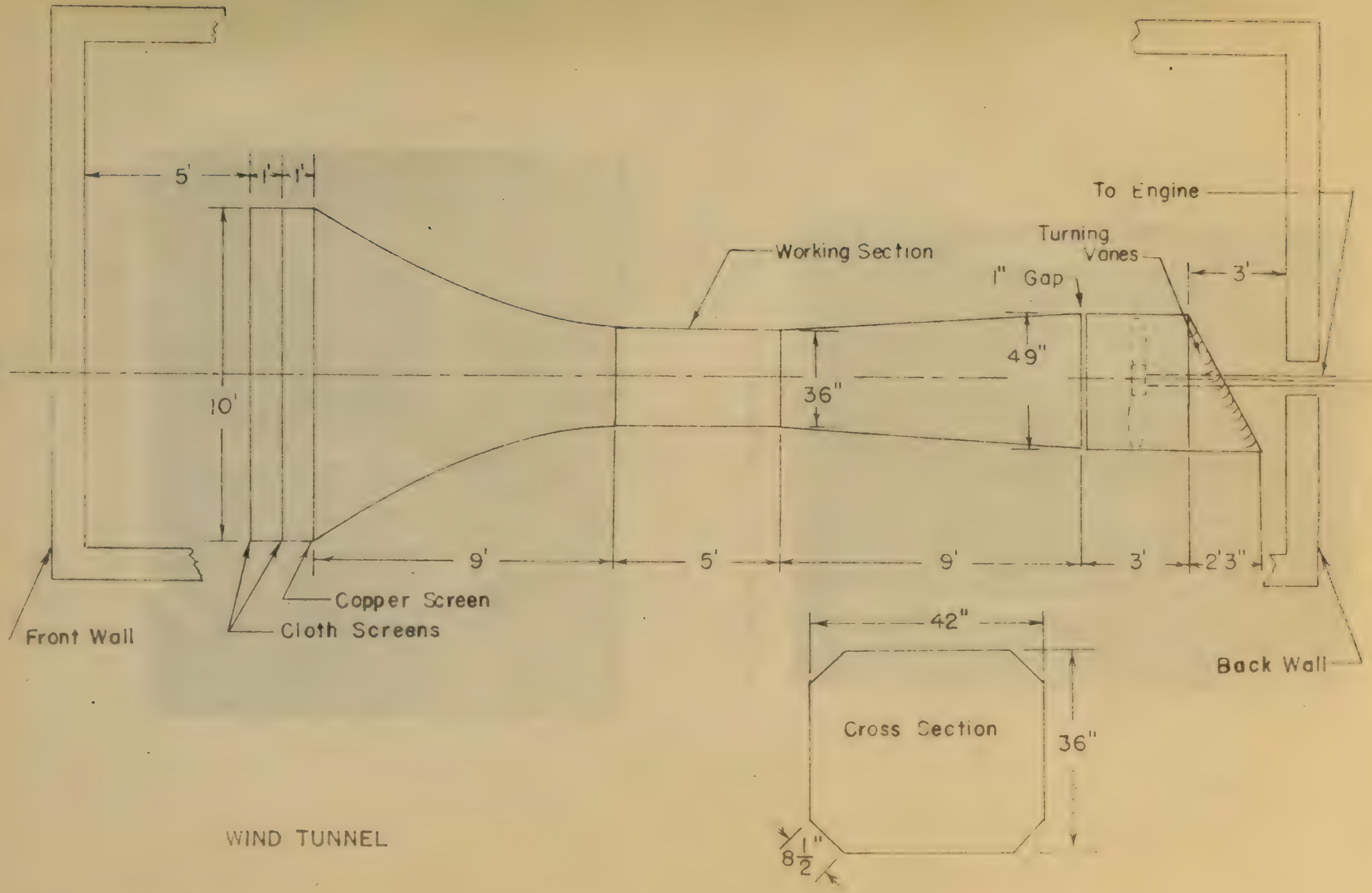

FIG. 1

WIND TUNNEL

a. Test section showing airfoil and barrier

b. Mounting bracket and flexure

Fig. 2

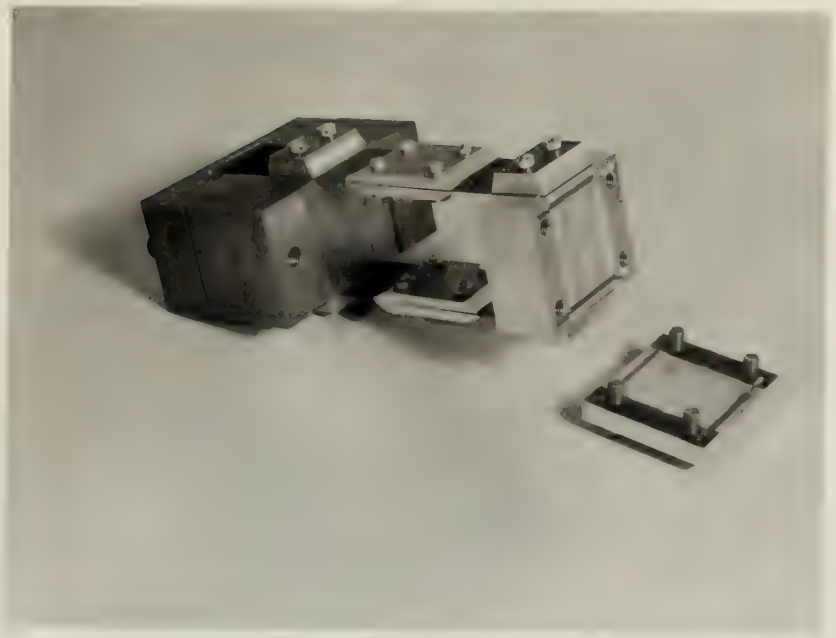

a. Flexure and spring clamp

b. Weights attatched to spring

Fig. 3

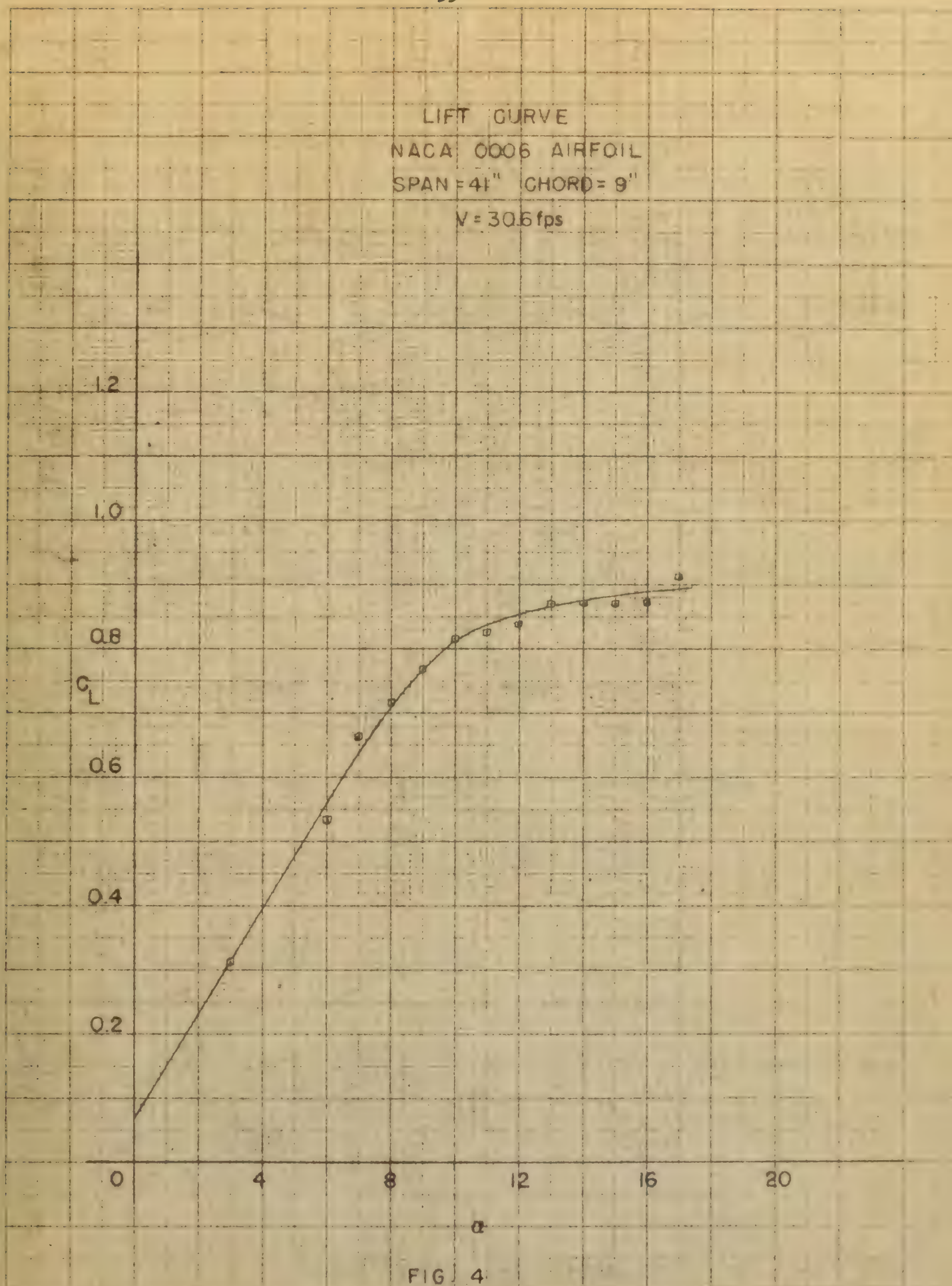
LIFT CURVE
NACA 0006 AIRFOIL
SPAN = 41" CHORD = 9"
V = 30.6 fps
1.2
1.0
0.8
C_L
0.6
0.4
0.2
0
4
8
12
16
20
α

FIG 4

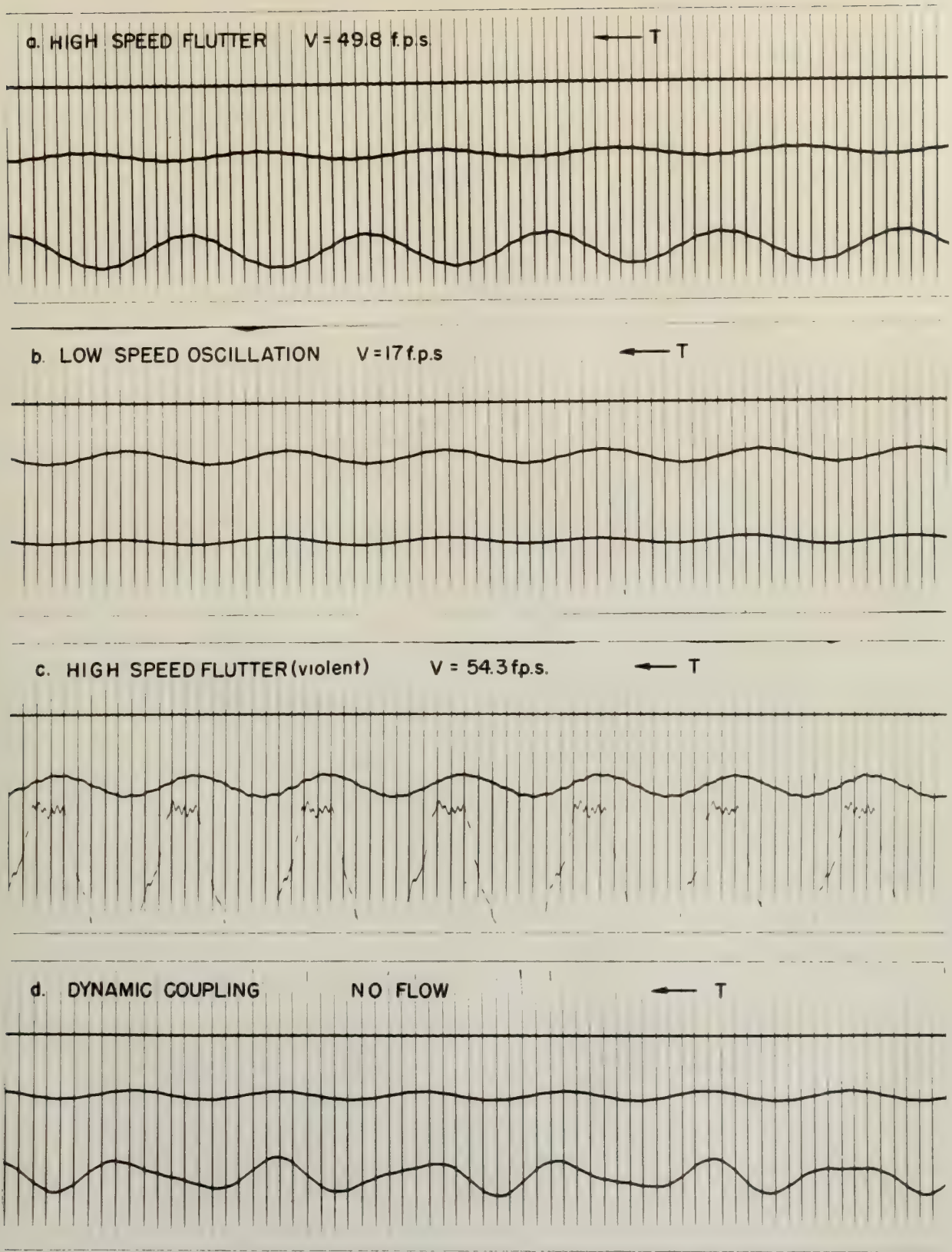

Sample Osillograph Recordings

Fig. 5

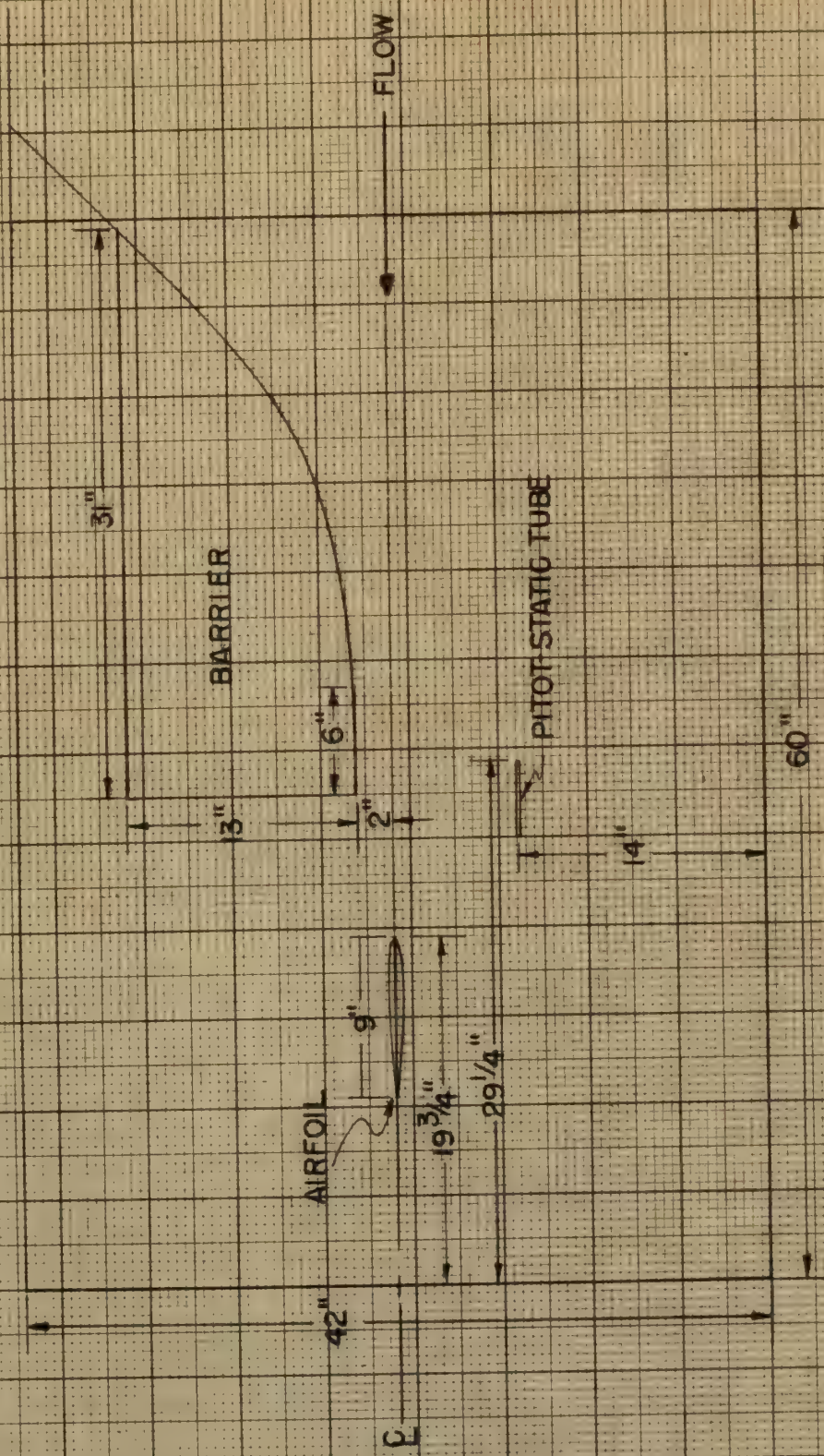

PLAN VIEW OF TEST SECTION

FIG. 6

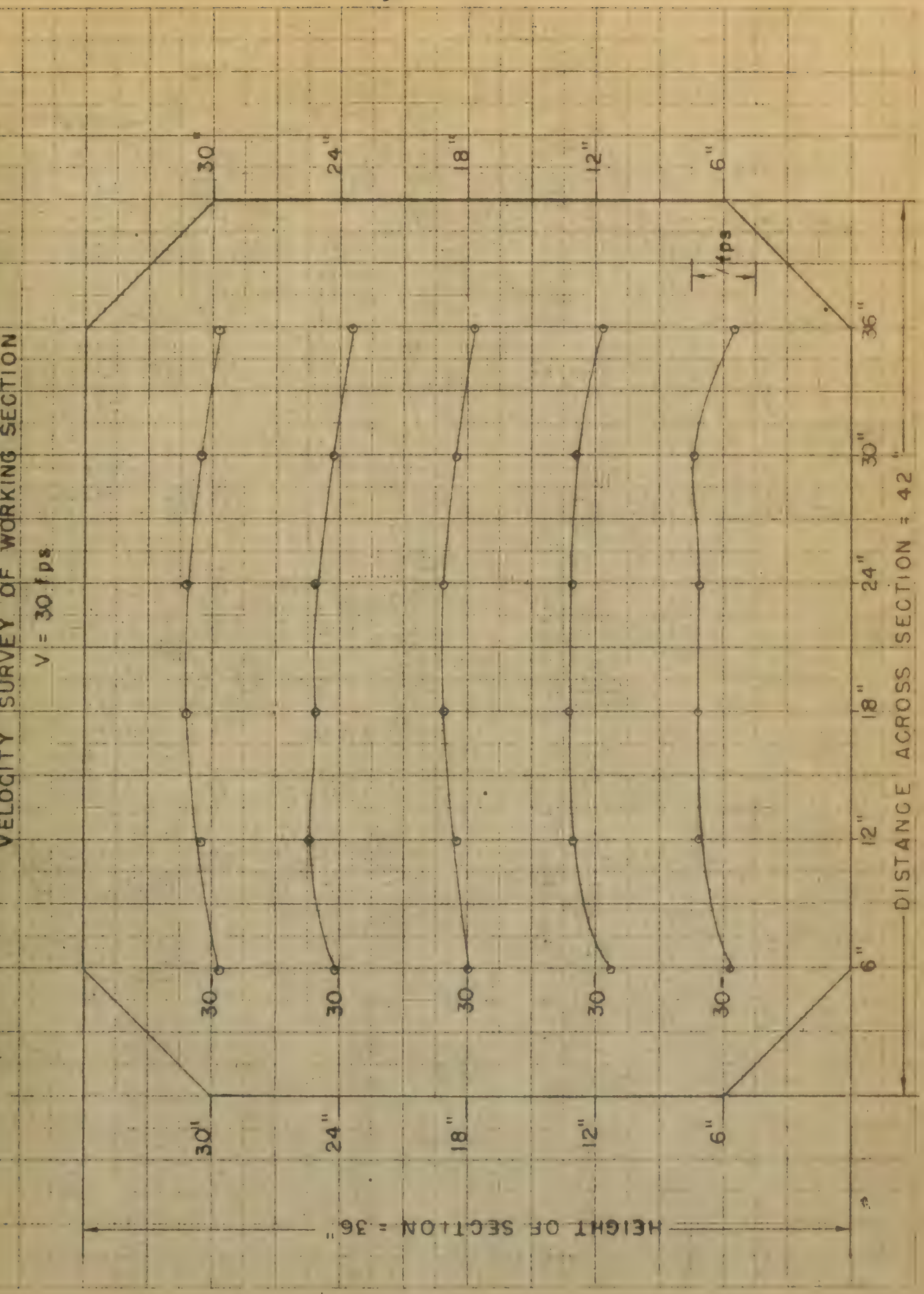
VELOCITY SURVEY OF WORKING SECTION
V = 30 fps
30"
24"
18"
12"
6"
1 fps
30
DISTANCE ACROSS SECTION = 42"
HEIGHT OF SECTION = 36"

FIG. 7

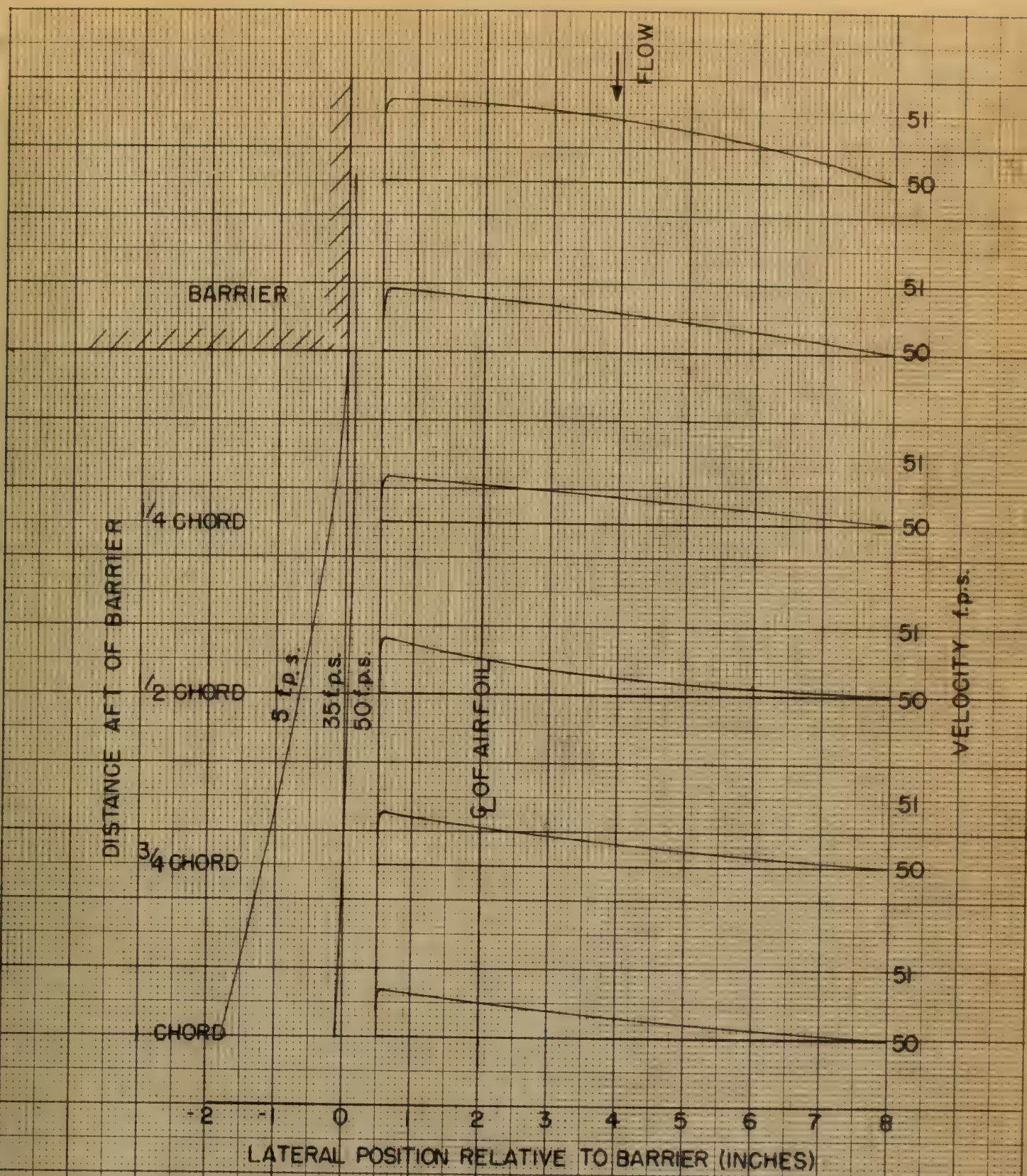

VELOCITY SURVEY AT 50 f.p.s.
(12" ABOVE TEST-SECTION FLOOR)

FIG. 8

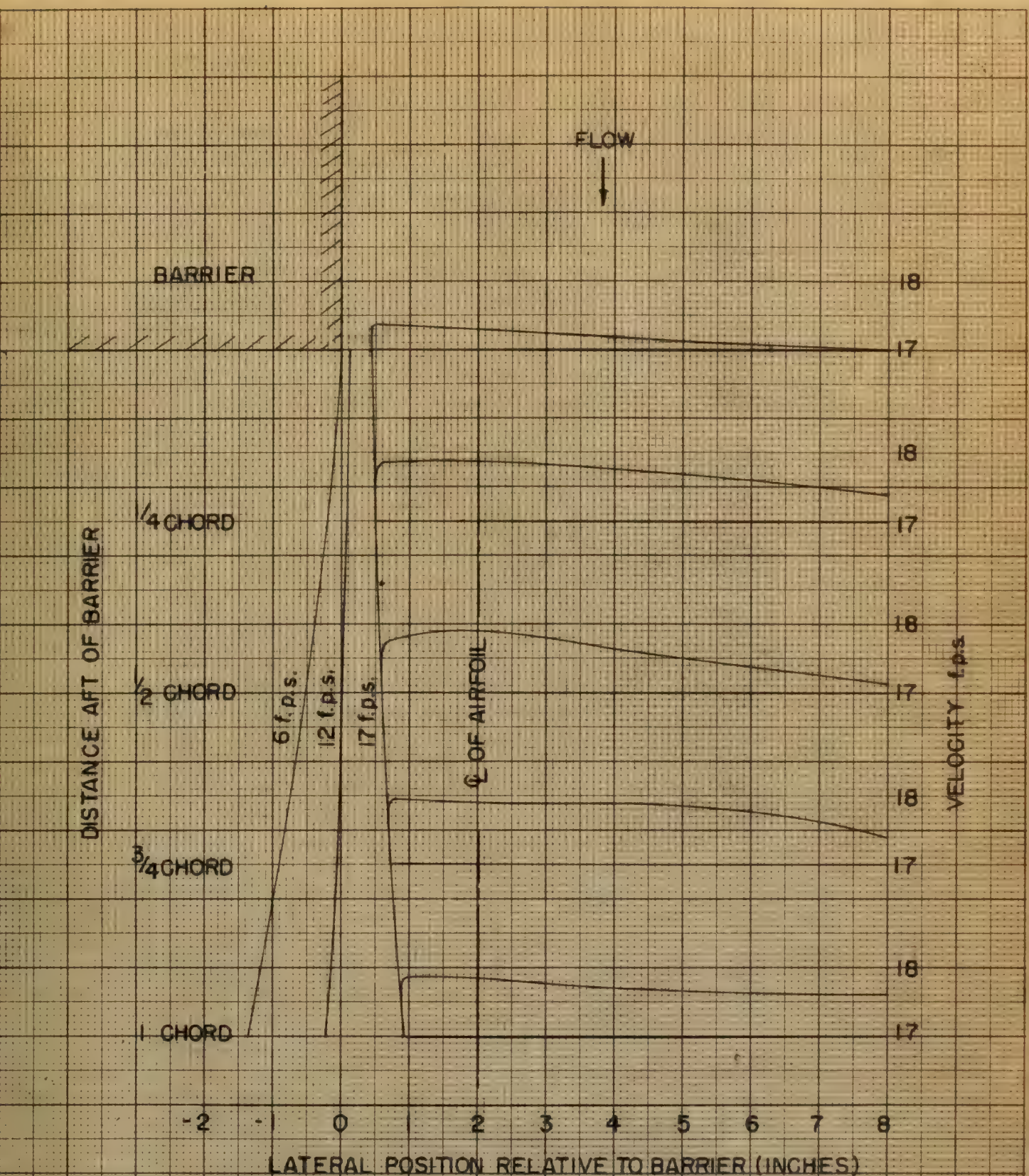

VELOCITY SURVEY AT 17 f.p.s.
(12" ABOVE TEST SECTION FLOOR)

FIG. 9

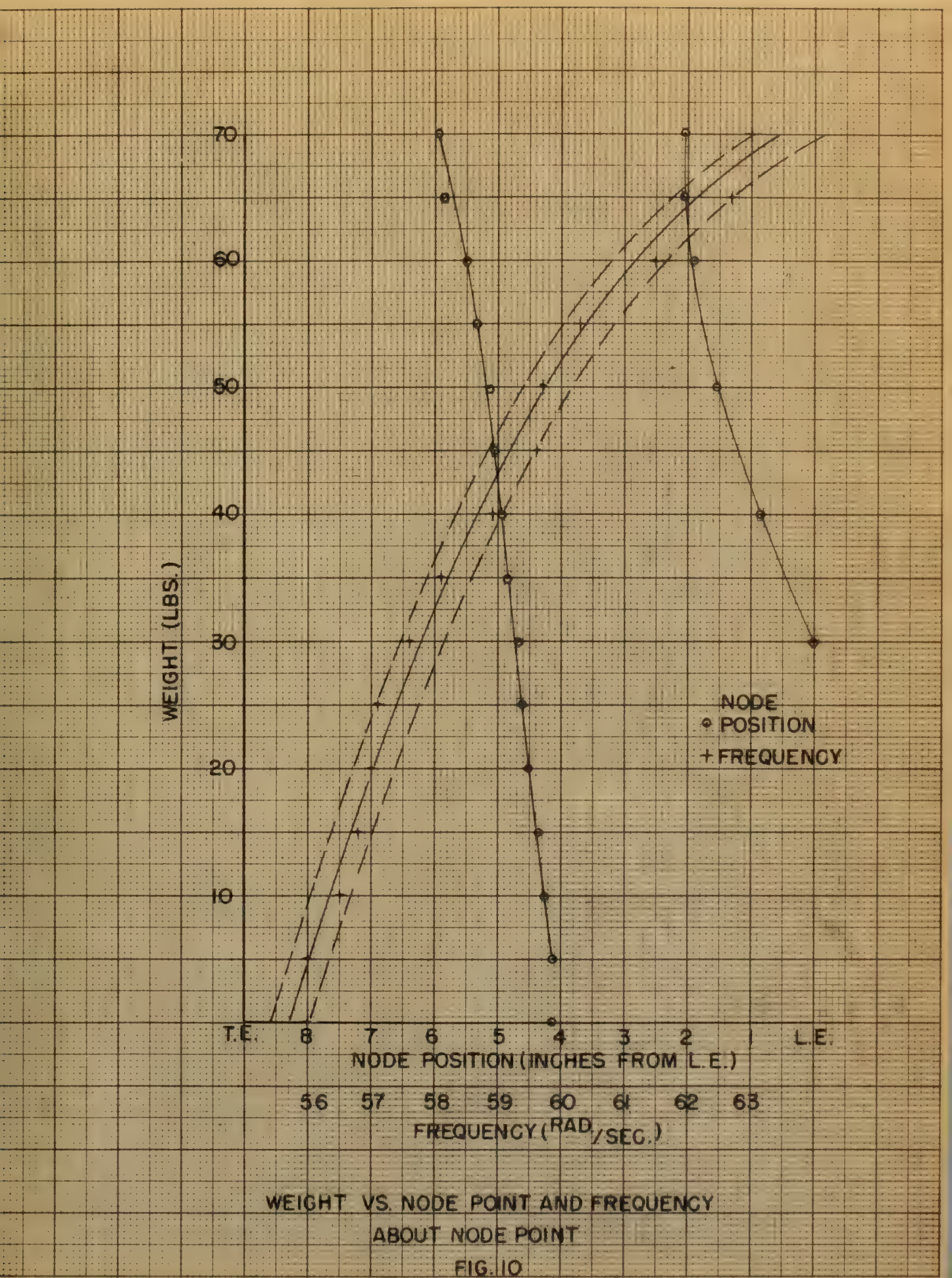

WEIGHT VS. NODE POINT AND FREQUENCY
ABOUT NODE POINT
FIG. 10

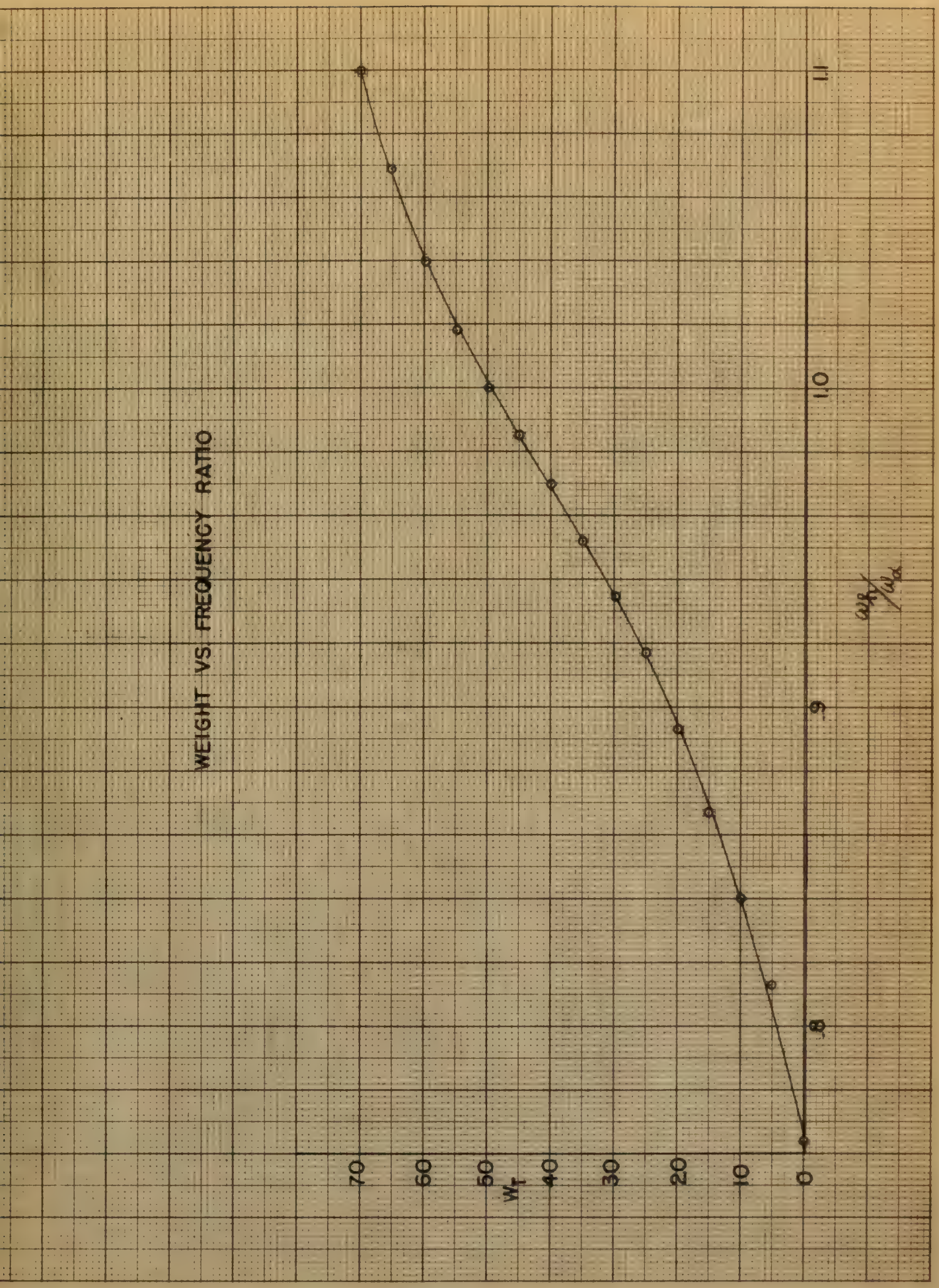
WEIGHT VS FREQUENCY RATIO
W_T
70
60
50
40
30
20
10
0
.8
.9
1.0
1.1
ω_R/ω_n

FIG. II

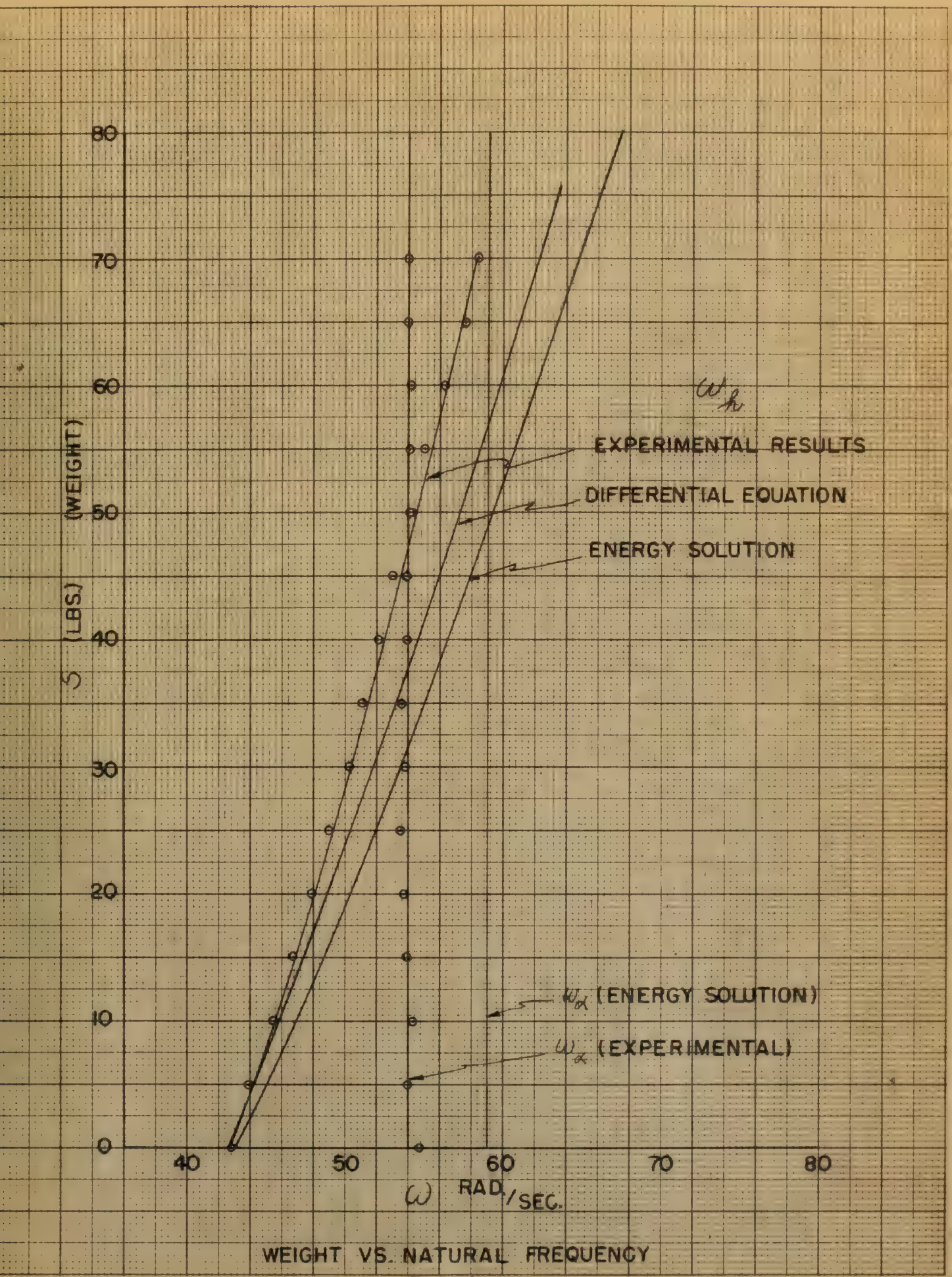

WEIGHT VS. NATURAL FREQUENCY

FIG. 12

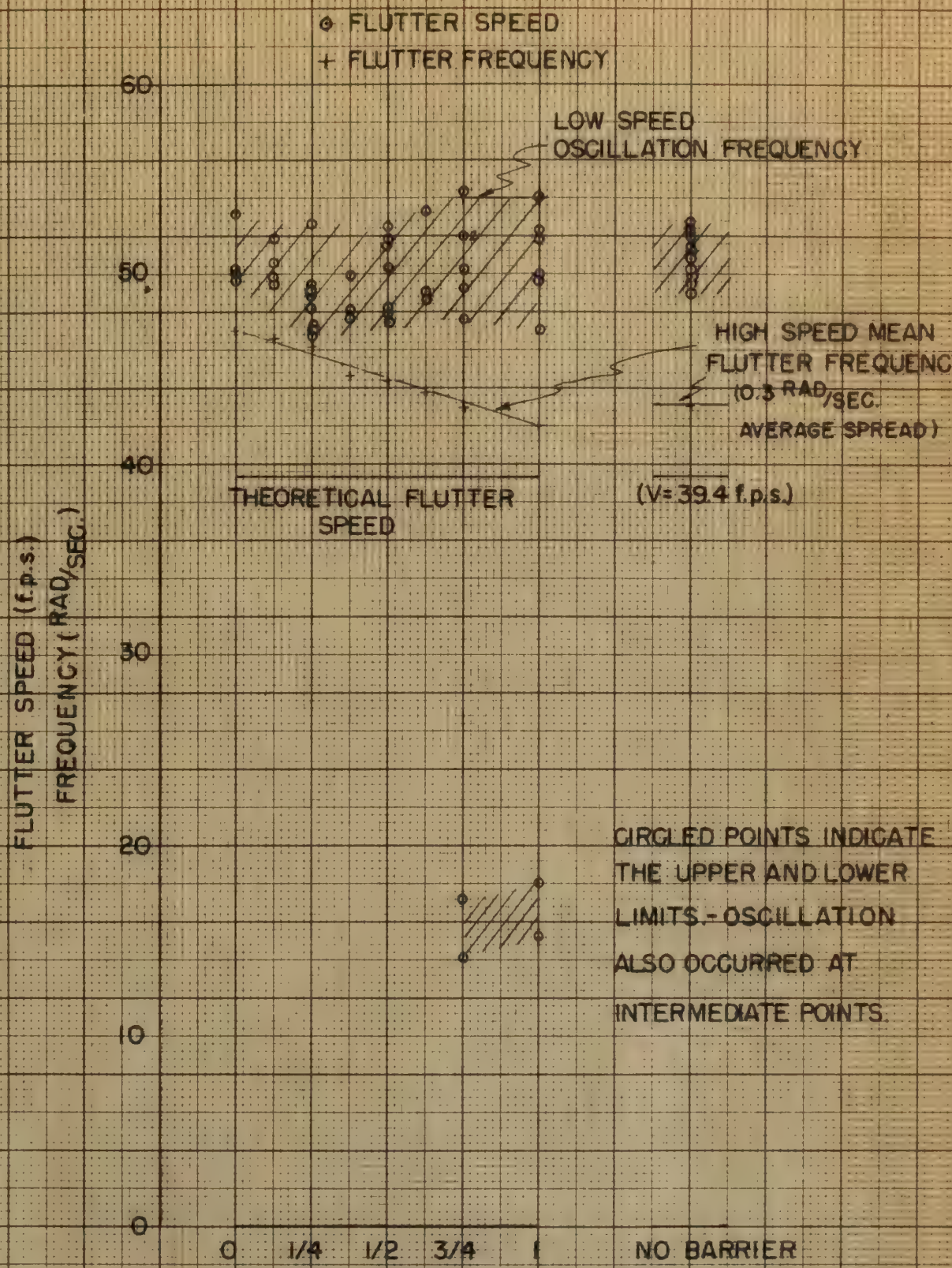

EXPERIMENTAL FLUTTER SPEEDS AND FREQUENCIES
FOR VARIOUS BARRIER POSITIONS

FIG. 13

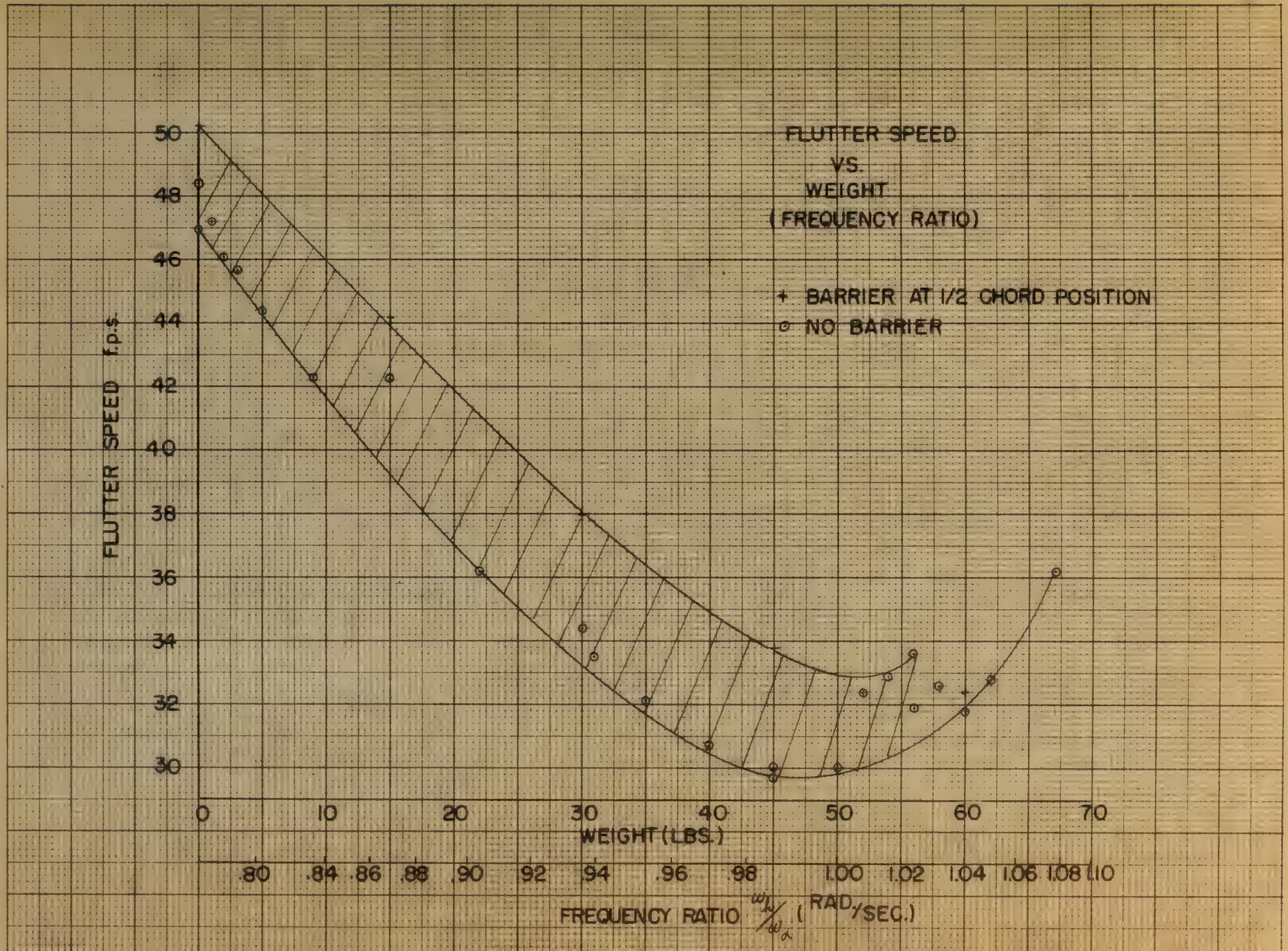
FLUTTER SPEED
VS.
WEIGHT
(FREQUENCY RATIO)
+ BARRIER AT 1/2 CHORD POSITION
⊙ NO BARRIER
FLUTTER SPEED f.p.s.
50
48
46
44
42
40
38
36
34
32
30
0
10
20
30
40
50
60
70
WEIGHT (LBS.)
.80
.84
.86
.88
.90
.92
.94
.96
.98
1.00
1.02
1.04
1.06
1.08
1.10
FREQUENCY RATIO ω_h/ω_α (RAD/SEC.)

FIG. 14

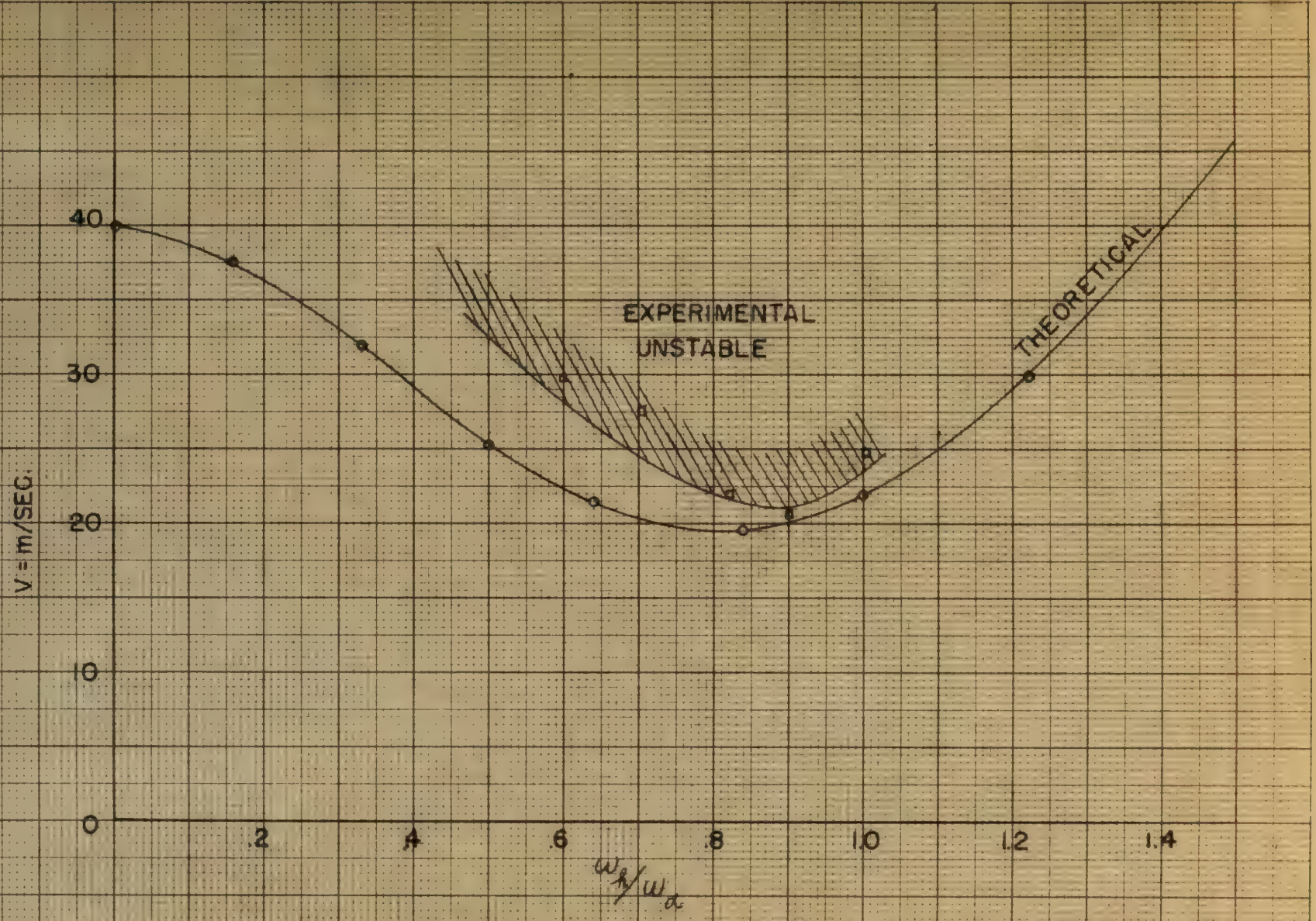

FIG. 15

THEORETICAL AND EXPERIMENTAL CURVES GIVING FLUTTER VELOCITY V AGAINST FREQUENCY RATIO ω_h/ω_α DEFLECTION-TORSION

Reproduced from Fig. 15 NACA Report No. 496, 1940

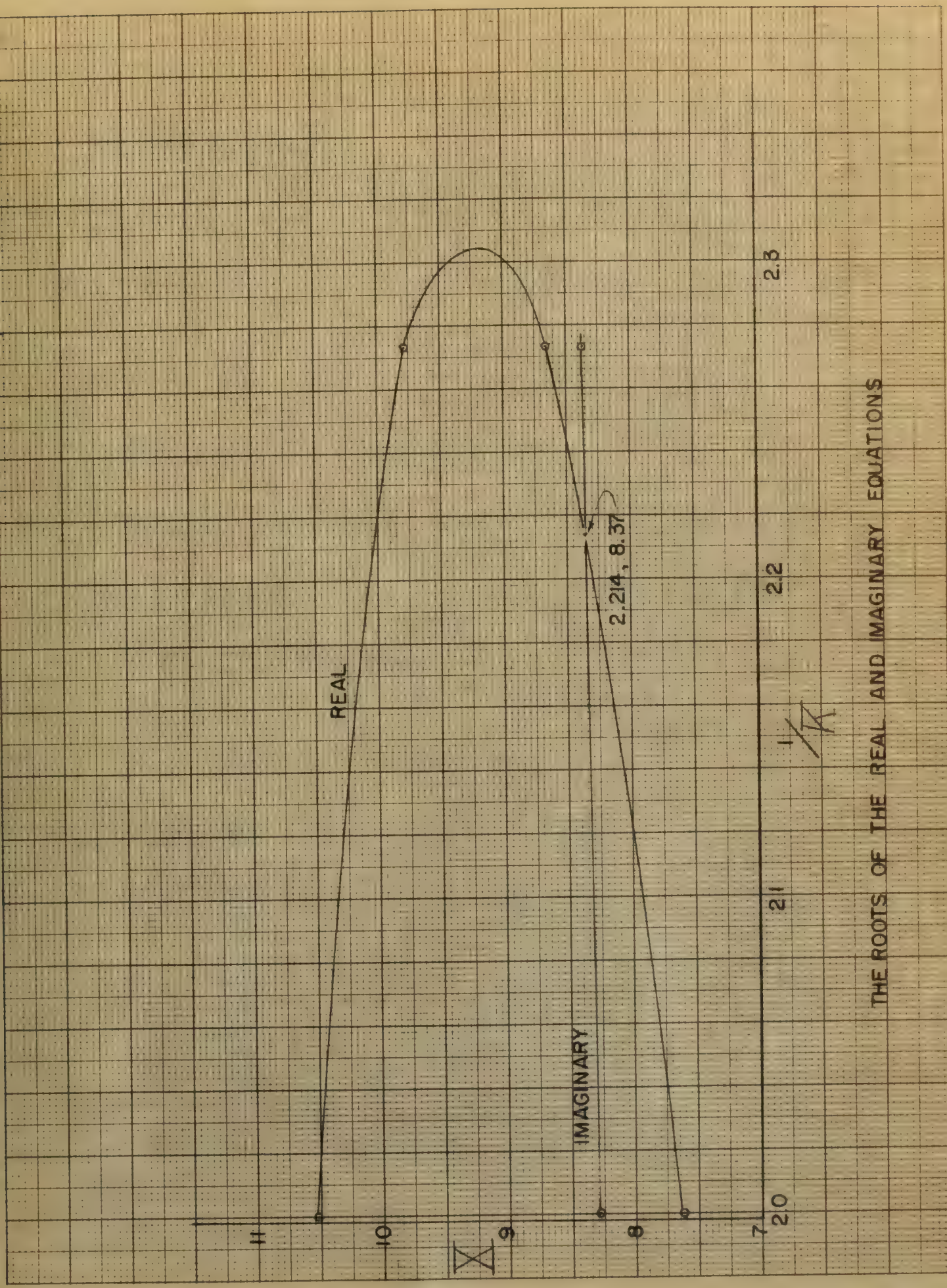
THE ROOTS OF THE REAL AND IMAGINARY EQUATIONS
REAL
IMAGINARY
2.214, 8.37
2.3
2.2
2.1
2.0
11
10
9
8
7
1/K
X

FIG. 16